frontiers | Frontiers in Marine Science

ORIGINAL RESEARCH
published: 17 June 2022
doi: 10.3389/fmars.2022.900679

Coral Reef Coupling to the Atmospheric Boundary Layer Through Exchanges of Heat, Moisture, and Momentum: Case Studies From Tropical and Desert Fringing Coral Reefs

Hamish McGowan[1]*, *Nadav G. Lensky*[2,3], *Shai Abir*[2,3] *and Melissa Saunders*[1]

[1] Atmospheric Observations Research Group, The University of Queensland, Brisbane, QLD, Australia, [2] Geological Survey of Israel, Jerusalem, Israel, [3] Hebrew University of Jerusalem, Jerusalem, Israel

Coral reefs represent abrupt changes in surface roughness, temperature, and humidity in oceanic and coastal locations. This leads to formation of internal atmospheric boundary layers that grow vertically in response to turbulent mixing which conveys changes in surface properties into the prevailing wind. As a result, coral reefs under favourable conditions couple to the overlying atmosphere. Here we present rare observations of coral reef – atmospheric interactions during summer monsoon conditions on the Great Barrier Reef, Australia, and a desert fringing coral reef in the Gulf of Eilat, Israel. We show that in the hyper-arid location of the Gulf of Eilat where air temperatures are greater than water temperatures, a stable atmospheric boundary inhibits coupling of the reef to the atmosphere. In contrast, under monsoon conditions on the Great Barrier Reef, the coral reef is shown to couple to the overlying atmosphere leading to the formation of a convective internal boundary layer in which convective exchange of heat and moisture influences cloud and possibly precipitation. We conclude that understanding these processes is essential for determining the role of coral reefs in coastal meteorology, and whether through coupling with the overlying atmosphere coral reefs may regulate their meteorology by triggering formation of cloud and/or vertical exchange on aerosols and their precursor gases such as Dimethyl sulphide.

Keywords: atmosphere, energy balance, Great Barrier Reef, Gulf of Eilat, cloud, boundary layers

OPEN ACCESS

Edited by:
Graham Barry Jones,
Southern Cross University, Australia

Reviewed by:
Steven Siems,
Monash University, Australia
Małgorzata Kitowska,
Polish Academy of Sciences, Poland

***Correspondence:**
Hamish McGowan
h.mcgowan@uq.edu.au

Specialty section:
This article was submitted to Coral Reef Research, a section of the journal Frontiers in Marine Science

Received: *21 March 2022*
Accepted: *19 May 2022*
Published: *17 June 2022*

Citation:
McGowan H, Lensky NG, Abir S and Saunders M (2022) Coral Reef Coupling to the Atmospheric Boundary Layer Through Exchanges of Heat, Moisture, and Momentum: Case Studies From Tropical and Desert Fringing Coral Reefs. Front. Mar. Sci. 9:900679. doi: 10.3389/fmars.2022.900679

INTRODUCTION

Coral reefs represent pronounced transitions in water temperature, roughness and humidity in coastal and oceanic settings. These changes propagate vertically into the atmosphere leading to formation of convective internal atmospheric boundary-layers (CIBL) within the marine atmospheric boundary layer (MBL) (Garratt, 1990; Garratt, 1994). The magnitude of coral reef coupling to the atmosphere through air-sea exchanges of sensible (Qh) and latent heat flux (Qe),

and momentum flux (τ) is dependent on time of day, season, and prevailing synoptic meteorology as observed over land in CIBLs (Garratt, 1990; Mahrt, 2000). Additionally, over coral reefs, tides influence water temperature with midday to afternoon low tides typically coinciding with higher daytime water temperatures, while high tides bring cooler ocean water over coral reefs. In oceanic settings, the shallower water of coral reefs results in reduced wave height and surface roughness, potentially causing higher windspeeds. For example, MacKellar et al. (2012a) reported roughness lengths for Heron Reef on the southern Great Barrier Reef (GBR), Australia of 0.00018 to 0.00038 m compared to values often quoted for deeper ocean water which may range from 0.0002 to 0.006 m (Golbazi and Archer, 2019; He et al., 2021). Fringing coral reefs bordering coasts may also experience acceleration of wind as air moves from the aerodynamically rough land to the smoother water surface during offshore flow (Garratt, 1990; Vickers et al., 2001). At low tide, exposed reef rims and reef flats where coral bommies and debris from tropical storms surmount the reef, the frictional effects of the reefs surface on the lower atmosphere are greatest causing turbulence. Collectively, such surface heterogeneity over coral reefs is likely to influence the vertical diffusion of heat, water vapour, aerosols, and gases such as CO_2 and Dimethyl sulphide (DMS).

DMS is a naturally occurring aerosol precursor gas, which can be produced by corals and their symbionts. DMS affects the global sulphur budget and aerosol formation which it has been claimed may modify climate through direct and indirect forcing of the surface radiation budget (Charlson et al., 1987). Cropp et al. (2018) considered such bioclimatic feedback as a potential defence mechanism against thermal stress induced coral bleaching. Observations from One Tree Reef on the southern GBR by Broadbent and Jones (2006) found the highest concentrations were recorded during summer, while Swan et al. (2016) at nearby Heron Reef observed DMS peaks coincided with low tides and low wind speeds as did Cropp et al. (2018). However, recent numerical modelling by Fiddes et al. (2021a) using the coupled climate–chemistry model ACCESS-UKCA, found no clear evidence that coral reef derived DMS has any significant impact on the meteorology of coral reefs. A subsequent study by Fiddes et al. (2022) using the WRF-Chem model also found no impact by local DMS over the GBR. They suggested air contaminants from terrestrial sources where more influential in addition to aerosolised sea salt emissions and their impact on atmospheric turbidity and cloud microphysics.

The influence coral reefs exert on the overlying atmosphere is dependent on exchanges of energy, aerosol, and gases across their air-sea interfacial boundary, and then through the CIBL. CIBL formation above coral reefs which MacKellar et al. (2013) named the convective reef layer (CRL) occurs within the marine boundary layer (MBL) in response to air-sea turbulent flux exchanges. MacKellar et al. (2013) observed the CRL to develop in response to positive surface turbulent energy fluxes, particularly heat (Qh) causing the near surface reef atmospheric boundary layer to transition from a stable nocturnal early morning profile to an unstable daytime profile from mid-morning. Clayson and Edson (2019) using satellite and buoy data from the Gulf Stream and Kuroshio Extension found a diurnal cycle in mean wind speeds which were faster and more humid over warmer SSTs. They hypothesised this was the result of greater latent heat (Qe) exchange caused by winds entraining moisture. Accordingly, CRL development can be considered analogous to a terrestrial CIBL, where following sunrise downwelling shortwave (solar) radiation increases the surface temperature resulting in an increase in Qh. Resulting convective diffusion of Qh and Qe, as well as entrained gases and aerosols subsequently occur as wind speeds increase causing additional turbulent mixing.

Here we present observations from the humid tropical/subtropical Heron Reef on the southern GBR, Australia and the fringing coral reef bordering the hyper-arid desert of the northern Gulf of Eilat (GoE), Israel of air – sea exchanges of turbulent energy fluxes, associated meteorology and atmospheric boundary layers. These rare observations begin to shed light on the meteorology of coral reefs in different climatic zones and their influence on the overlying atmosphere. They are essential to inform debate on the role of coral reefs in marine and coastal meteorology and possible bioclimatic feedback processes such as cloud development. Recommendations for future research priorities are then made to advance understanding of the role of coral reefs in local to mesoscale meteorology.

RESEARCH SETTINGS – HERON REEF AND GULF OF EILAT

Heron Reef is located on the southern GBR, Australia (**Figure 1D**) and the desert fringing coral reef in the northern GoE, Israel (**Figure 1A**). The contrasting meteorology of these two locations being a humid marine tropical/subtropical environment and coastal hyper-arid location respectively, represent extremes in heat and moisture experienced by coral reefs and their air-sea exchanges of sensible and latent heat fluxes.

Heron Reef

Heron Reef is one of more than 2,900 coral reefs that make up the GBR, the world's largest emergent reef system covering ~345,950 km^2 (Woodroffe, 2003). It is located on the southern GBR around 80 km northeast of the township Gladstone on the northeast coast of Australia. The reef is a typical lagoonal platform reef covering ~27 km^2, as it extends south-eastward from Heron Island, which is located on the northwest margin of the reef (**Figure 1D**). Annual rainfall at Heron Reef is ~1,050 mm, with the majority of precipitation occurring during summer (December to February) coinciding with the Australian monsoon, and in autumn (March to May). June to September is the driest period of the year when anticyclones track east across the Australian continent and bring mostly calm and settled conditions to the area. The wind regime of Heron Reef is dominated by the south-easterly trade winds, while wind direction becomes more variable in summer with the

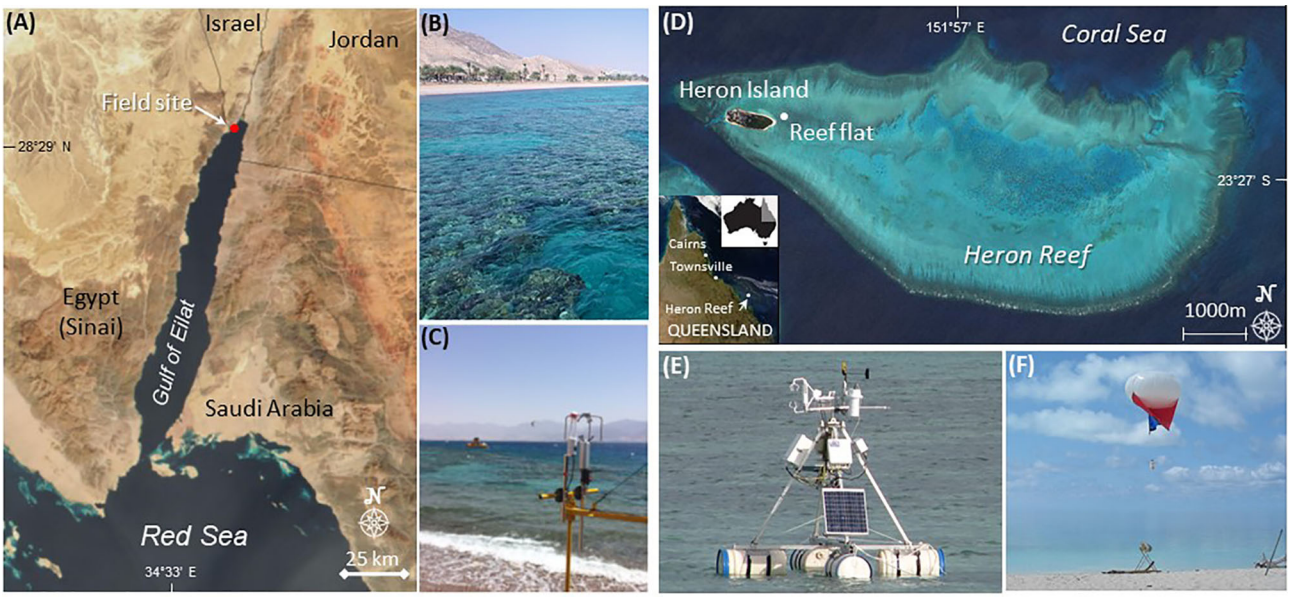

FIGURE 1 | Gulf of Eilat location map (*Google Earth*, earth.google.com/web/) and eddy covariance field site **(A)**; desert fringing coral reef, Eilat **(B)**; shoreline eddy covariance system, Eilat **(C)**; Heron Reef location map (Satellite image from the Ikonos satellite provided by DigitalGlobe and Centre for Spatial Environmental Research) with reef flat eddy covariance site indicated **(D)**; pontoon eddy covariance system, reef flat, Heron Reef **(E)**, helikite sounding system on shore of Heron Reef **(F)**.

occurrence of occasional strong northeasterlies, although south-easterly winds still dominate. The strongest winds are associated with the passage of tropical cyclones during the summer. The highest mean daily maximum air temperature occurs in January at 29.8°C, with the lowest mean daily minimum air temperature in July at 16.7°C (McGowan et al., 2010; MacKellar et al., 2012a).

The major geomorphic zones on Heron Reef are the reef flat, shallow, and deep lagoons which, respectively, cover 32%, 16%, and 12% of the total reef surface. The remaining area of Heron Reef is composed of the outer reef flat, reef slope, reef crest and the coral cay, which cover 20%, 13%, 6%, and 1%, respectively. The coral *Acropora* spp. is prevalent in the deeper waters of the reef system along with the massive corals *Porites* spp. on the reef flat. Heron Reef experiences semidiurnal tides with a spring and neap tidal range of 2.28 and 1.09 m (Chen and Krol, 1997). Wave height on the reef flat is typically <0.5 m under a mean wind speed of 5 ms^{-1}, and wave heights are <0.6 times the maximum water level (Gourlay, 1988). When the tide is higher than the reef rim, oceanic waves may travel across the reef flat, resulting in the regional wave climate being the key control of wave action. Occasionally, wind waves are superimposed on low to moderate sea swell produced by the prevailing south-easterly trade winds. Cyclonic storms during late summer that are concurrent with king tides may cause large waves to travel over the reef.

Gulf of Eilat

The GoE is an almost rectangular region roughly 6 × 10 km with steep lateral boundaries with a maximum depth of nearly 800 m (Carlson et al., 2012) in the northern Red Sea (**Figure 1A**). During the summer months, June-September, the lower level atmosphere in the region is dominated by the Persian Trough, which extends from the Asian monsoon region through the Persian Gulf (Alpert et al., 1990; Bitan and Sa'Aroni, 1992), generating winds from the northwest. Desert mountains located around the Ha'Arava Rift valley channel winds onto the northeast GoE with an average daytime speed of 5-7 m s^{-1} bringing hot and dry air.

The highest mean daily maximum air temperature occurs in July at 40°C with the lowest mean daily minimum air temperature occurring in January at 5.9°C. Annual mean total rainfall is 24 mm while >3350 hrs of sunshine occur highlighting the hyper-arid desert climate of the region. Mean daily water surface temperature (1988 to 2020) varies from around ~21°C during February to March (Shaked and Genin, 2020) peaking at ~28°C from July to September. Mean water depth at the field site from which measurements are discussed here on the northwest shoreline of the GoE over the reef table is 0.5 m. Mean tidal range during the observation period was 0.35 m, with a semi-diurnal cycle.

Coral coverage area is 28%, rock 15%, dead coral 10% and the remainder being substrate comprised of sand and shell fragments (Shaked and Genin, 2019). Coral taxa along the coast is highly diverse with the back-reef lagoon dominated by *Stylophora pistillata*, while in the forereef more than 40 coral genera are regularly identified, with the most common comprising of *Stylophora*, *Acropora*, *Montipora*, *Echinopora*, *Cyphastrea*, *Goniastrea*, *Porites* and *Dipsastrea*. Coral coverage averages approximately 25% with rock making up around 20%, dead coral 5% and the remaining being loose substrate of sand and shell fragments (Shaked and Genin, 2020) (**Figure 1B**). The shoreline current is predominantly from north to south in

response to prevailing northerly winds, with a semidiurnal and diurnal barotropic tide range of around 1 m (Shaked and Genin, 2019).

CORAL REEF – ATMOSPHERE FORCINGS

Reefs in the Humid Tropics/Subtropics: Case Study Heron Reef

Direct measurements air-sea energy exchanges over Heron Reef were made using an eddy covariance (EC) system mounted on a pontoon (MacKellar et al., 2013; McGowan et al., 2019) (**Figure 1E**). The EC included a Campbell Scientific CSAT-3 sonic anemometer, Li-Cor CS7500 open-path H_2O and CO_2 analyzer, a Kipp and Zonen CNR1 net radiometer (NR-Lite net radiometer by Kipp & Zonen) with additional sensors measuring water and air temperature, atmospheric pressure and relative humidity (MacKellar et al., 2012a; MacKellar et al., 2013). The EC instruments were controlled by a Campbell Scientific CR23X data logger with measurements made at 10 Hz with 15 minutes block averages recorded. Vertical profiles up to ~500 m asl. of air temperature, humidity, wind speed and direction were obtained using a Kestrel 4500 weather monitor tethered to a kite when wind speeds exceeded 5 ms^{-1}, or to a helium-inflated Helikite (**Figure 1F**) at lower wind speeds with measurements logged every 10 s (MacKellar et al., 2013). In 2009 a Vaisala ceilometer CL31 was also deployed at Heron Island to monitor cloud, aerosol and boundary layer height (Kotthaus et al., 2016) with a vertical measurement resolution of approximately 10 m.

Fair Weather Air-Sea Exchanges

Measurements of the daytime surface energy balance by EC over the reef flat on Heron Reef (151°55.203 E, 23°26.573 S) were made on the 4 February 2008 under settled fair weather conditions associated with a ridge of high pressure extending along the east Australian coast (**Figure 2A**). Winds were light ranging from 2 to 5 ms^{-1} with cloud cover varying throughout the day from 4/8 to 8/8 consisting of stratocumulus, cirrostratus in the morning with embedded cumulus in the prevailing easterly airstream. Review of available satellite imagery showed

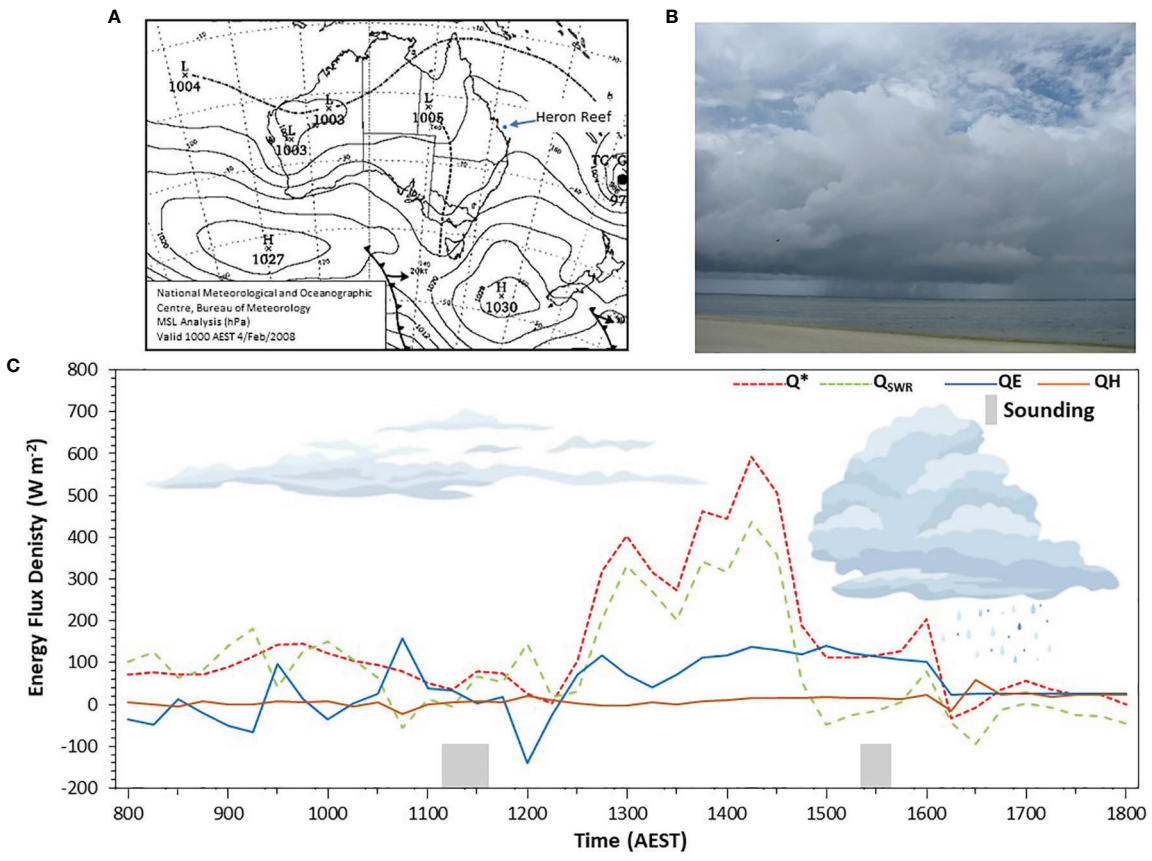

FIGURE 2 | Mean Sea Level Analysis 1000 AEST, 4 February 2008 **(A)**; photograph of convective shower approaching Heron Reef, 1524 AEST, 4 Feb 2008 **(B)**; daytime eddy covariance energy flux measurements made over the reef flat, Heron Reef with timing of tethersonde soundings shown with major cloud types **(C)**.

the cumulus cloud field becoming more significant in proximity to the southern GBR resulting in isolated convective showers in the afternoon at Heron Reef (**Figure 2B**).

The surface energy balance measured on the 4 February 2008 reflected the impact of mid-level cloud cover in the morning from 0800 AEST [Australian Eastern Standard Time (UTC +10 hrs)] to 1200 AEST with net radiation (Q*) ranging from ~10 to ~145 Wm^{-2} before increasing after midday (**Figure 2C**). Sensible heat flux (Qh) remained mostly constant throughout the day within the range of ~ -23 to ~59 Wm^{-2}, while Qe varied from positive to negative values during the morning before becoming mainly positive (evaporation) from midday to late afternoon (**Figure 2C**). Heat flux into the water and benthos (Q_{SWR}) was mostly positive averaging 351 Wm^{-2} hr between 0800 AEST to 1200 AEST, then 838 Wm^{-2} hr between 1215 to 1500 AEST before becoming negative between 1515 AEST to 1800 AEST averaging -69 Wm^{-2} hr. There was a net gain of energy to the reef flat between 0800 AEST to 1800 AEST on the 4 February 2008 of 371 Wm^{-2} hr. This caused water temperature to increase from 26.1°C at 0800EST to a maximum of 28.6°C at 1515 AEST and contributed to an increase in air temperature as shown in the tethersonde profiles in **Figure 3**.

Tethersonde profiles of wind speed, virtual potential temperature (θ_v) and mixing ratio were collected from 1110 to 1136 AEST (**Figures 3A–C**) and 1525 to 1536 AEST (**Figures 3D–F**). The late morning sounding displayed a well-mixed θ_v profile indicating a statically neutral lower atmosphere (**Figure 3A**) with a mixing ratio profile showing a moist surface layer ~70 m deep which we infer was the CRL caused by Heron Reef (positive Qe) below drier air above (**Figure 3B**). Wind speed was relatively constant in the CRL layer at ~5 ms^{-1} before gradually increasing through to the top of the profile at around 250 m (**Figure 3C**). In the second sounding from mid-afternoon the entire profile (~ 250 m) had warmed by 1 to 1.5°K and become weakly statically stable (**Figure 3D**). The mixing ratio profile showed an increase in moisture above the CRL (**Figure 3E**), while wind speed was very similar to that measured in the late morning profile (**Figure 3F**). The CRL was still evident in the mixing ratio profile with a maximum height of ~70 m. The photo of a convective shower moving onto Heron Reef at 1534 AEST (**Figure 2B**), highlights the change in conditions that occurred following maximum heating of the reef around 1300 to 1400 AEST with evaporation from the reef and adjacent ocean contributing to increased boundary layer

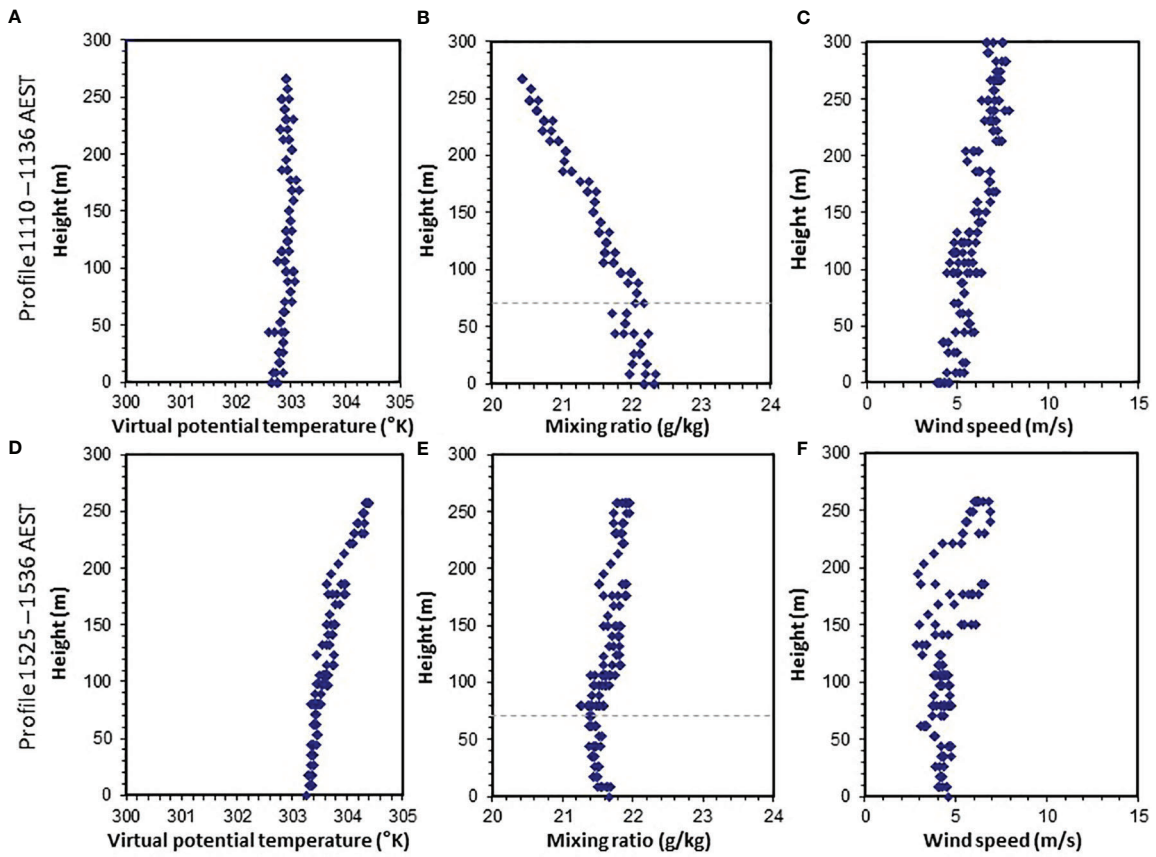

FIGURE 3 | Profiles of virtual potential temperature, mixing ratio and wind speed collected over Heron Reef, 4 Feb 2008 from 1110 – 1136 AEST **(A-C)** and 1525 – 1536 AEST **(D-F)**. Wind direction was consistent at around 95° giving a fetch of 7.64 km over the reef from the reef rim to the sounding site.

moisture and positive buoyancy with associated liberation of Qe following condensation resulting in convective showers.

Air-Sea Exchanges Under Monsoon Influences

The period 20 - 23 February 2009 was characterised by onset of monsoonal conditions at Heron Reef. Clear and settled weather with light winds prevailed on the 20 February due to a weak synoptic pressure gradient (**Figure 4A**). An inland surface trough was located over central Queensland, while the monsoon trough and weak tropical low were over the north Australian coast (**Figure 4A**). By the 22 February Heron Reef was under the influence of the east-southeast extension of the monsoon trough which had moved south into the Coral Sea and was located northeast of Heron Reef (**Figure 4B**). A ridge of high pressure along the southeast coast of Australia directed a warm moist easterly airstream onto Heron Reef (**Figure 4B**).

Surface energy balance measurements made over the reef flat (151°55.154 E, 23°26.617 S) under the increasing influence the Australian monsoon (20 to 23 February 2009) are presented in **Figure 4C**. These reflect clear sky conditions on the 20 February with Q* reaching a maximum of ~ 831 Wm^{-2} at 1215 AEST. Between 0600 AEST to 1800 AEST ~76% of Q* went into Q_{SWR} heating the water overlying the reef and underlying benthos and substrate. As a result, the reef flat water temperature increased from 26.3°C at 0600 AEST to a maximum of 34.4°C at 1600 AEST before decreasing slightly to 33.3°C at 1800 AEST as energy from the water was transferred to the atmosphere *via* evaporation (increased Qe and negative Q_{SWR}) (**Figures 4C, D**) as wind speed increased to

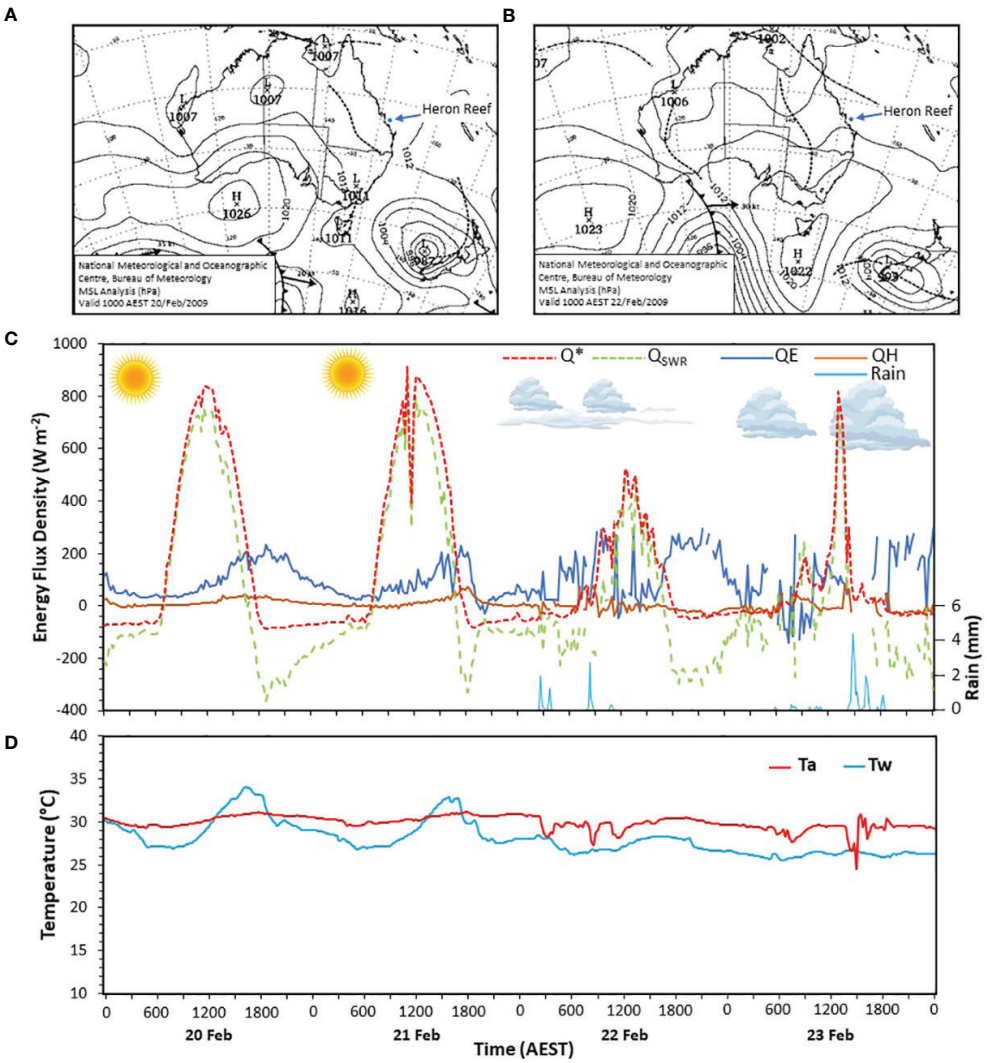

FIGURE 4 | Mean Sea Level Analysis 1000 AEST, 20 February 2009 **(A)** and 1000 AEST, 22 February 2009 **(B)**; with eddy covariance energy flux measurements (20 – 23 February 2009) made over the reef flat, Heron Reef and supporting meteorological observations **(C)**; and air and water temperature **(D)**.

around 4.5 ms^{-2}. Conditions on the 21 February were similar, but with cloud in the late morning causing a sharp decrease in Q* before it peaked in the early afternoon (**Figure 4C**). On the 22 February an increase in cloud cover reduced solar radiation receipt at the surface with Q* peaking at 512 Wm^{-2} at 1215 AEST. Showers affected Heron Reef throughout the morning as the monsoon trough moved south into the northern Coral Sea (**Figures 4B, C**). Water temperature decreased from 28.3°C in the early morning to around 26.6°C at 0600 AEST (**Figure 4D**) corresponding to onset of showers and an increase in wind speed to approximately 5 ms^{-2}. Water temperature then gradually increased to a maximum of 28.6°C at 1600 AEST before decreasing after 1800 AEST with 91% of Q_{SWR} lost *via* Qe and the residual to Qh (**Figures 4C, D**) as wind speeds peaked at 9.6 ms^{-2} in the late evening. Significant convective shower activity dominated the meteorology at Heron Reef on the 23 February with energy fluxes ranging between ~200 to -200 Wm^{-2} except for around 1330 AEST when Q* peaked briefly at 816 Wm^{-2} as skies cleared (**Figure 4C**). Wind speed reached a maximum of 10.4 ms^{-2} at 1600 AEST as convective showers passed over Heron Reef (**Figure 4C**) with Tw displaying a gradual decrease (**Figure 4D**). Air temperatures during the four-day period displayed a weak diurnal cycle on the 20 and 21 February reaching daytime maximums of around 30°C at 1800 AEST before trending down on the 22 and 23 February (**Figure 4D**). Down mixing of cooler air associated with the passage of convective showers over Heron Reef on the 22 and 23 February resulted in concurrent rapid decreases of Ta as shown in **Figure 4D**.

Figure 5 presents daily ceilometer backscatter plots for the 20 to 23 February 2009 from Heron Island (151°54'46.20" E, 23° 26'32.99" S). **Figure 5A** shows the backscatter plot for the 20

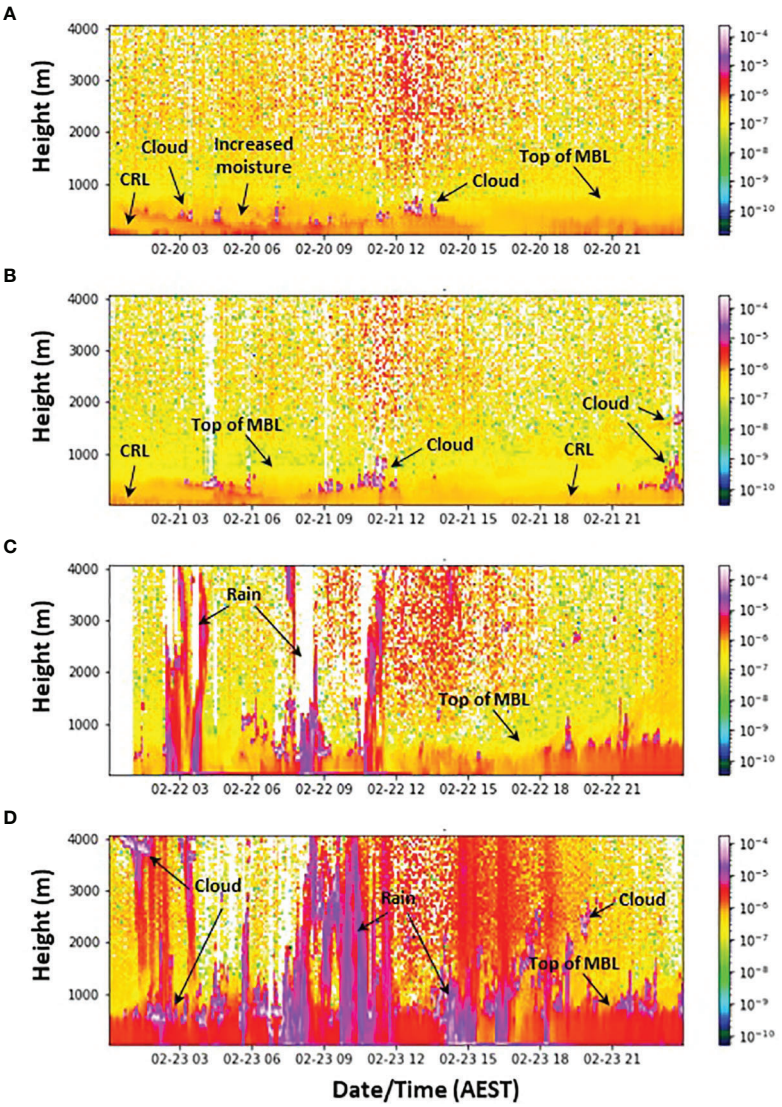

FIGURE 5 | Ceilometer reflectivity plots for the 20 **(A)**, 21 **(B)**, 22 **(C)** and 23 **(D)** February 2009. The ceilometer was installed on Heron Island (**Figure 1D**).

February when clear skies prevailed except for some isolated stratocumulus. A clear boundary in the reflectivity profile data at around 800 m asl we interpret as the top of the MBL. Below this, a layer of more humid air is evident, initially around 500 m asl. at 0100 AEST lowering to around 200 m asl. in depth at sunrise at 0600 AEST (**Figure 5A**). Isolated convective plume-initiated formation of cloud occurred during the day as highlighted in **Figure 5A**, while there was a very shallow surface layer of increased backscatter below 100 m asl which we interpret as the CRL. On the 21 February the top of the MBL lowered to ~600 to 700 m asl. (**Figure 5B**), while there was evidence of a shallow layer of increased backscatter in the lowest 100 m which we again interpret as the CRL. The presence of cloud can be seen in the ceilometer data before sunrise and then again through the morning to midday with a maximum height of approximately 1000 m asl. being mostly shallow cumulus. A layer of cirrostratus was also present but above 4000 m asl. (not shown). From mid-afternoon the top of the MBL becames less defined with the onset of cloud near 2400 hrs with a cloud base of 350 m, and cloud at 1800 m asl. (**Figure 5B**). The arrival of a more humid monsoon airmass on the 23 February resulted in convective showers affecting Heron Reef as previously discussed and seen in **Figure 5D**. The MBL ranged from ~700 to around 1000 m in depth, with increased moisture content into the evening as indicated by increased backscatter (**Figure 5D**). A lower cloud layer between ~600 to 1100m asl and other cloud layers between ~2000 m to > 4000m asl. were present on the 23 February with the ceilometer also identifying a layer of cirrostratus at around 6500 m asl (not shown).

Aerological profiles of temperature, humidity, wind speed and direction were obtained from the 20 – 23 February to maximum heights of around 500 m asl. (**Figure 6**). Vertical profiles of θ_v on the 20 February showed a warming through the morning and a transition to a statically unstable profile at 1445 AEST (**Figure 6A**). Subsequent cooling at the surface caused the lowest 100 m of the profile to cool by around 1°K by 1615 AEST

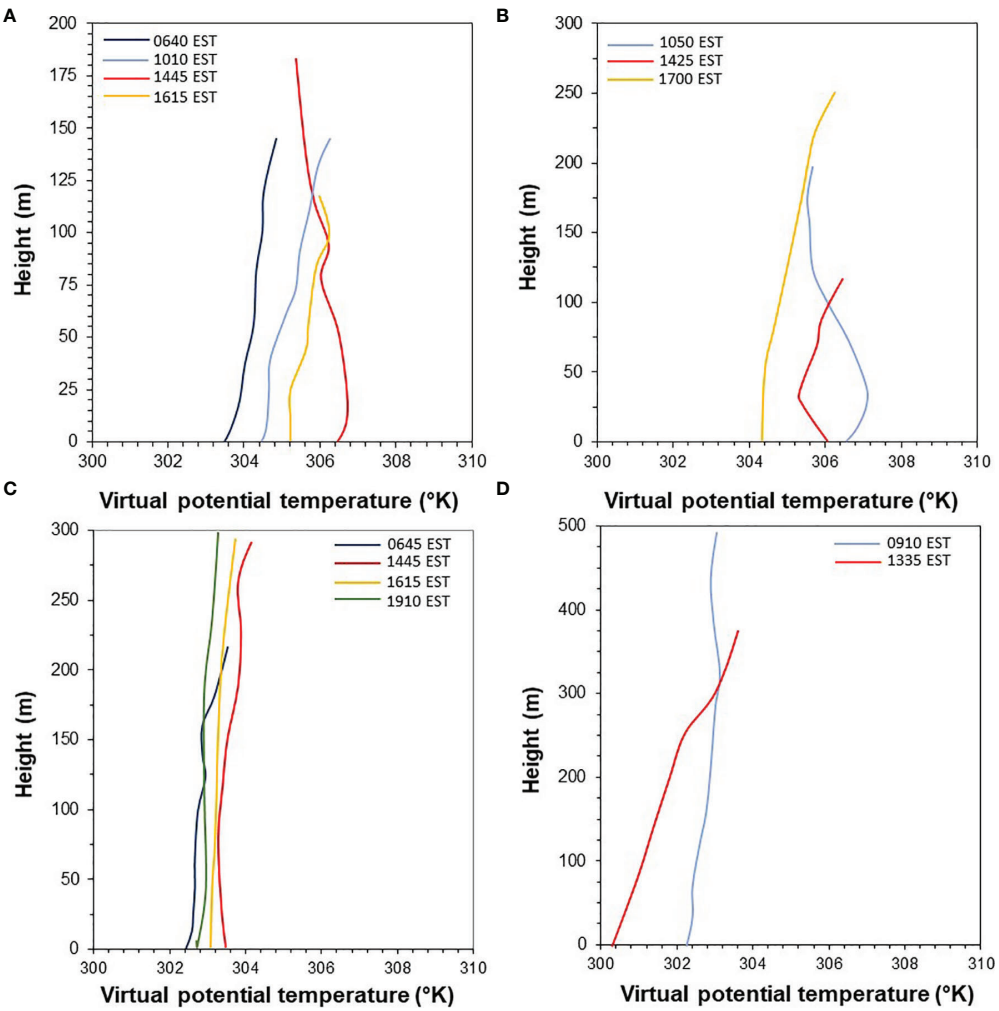

FIGURE 6 | Virtual potential temperature profiles collected over Heron Reef by tethersonde on the 20 **(A)**, 21 **(B)**, 22 **(C)** and 23 **(D)** February 2009.

leading to an increase in stability. This contributed to the absence of cloud as seen in the ceilometer data (**Figure 5A**). The θ_v profiles for the 21 February also display a cooling and increase in static stability from late morning through to late afternoon in the lowest 150 m (**Figure 6B**) which likely inhibited cloud development over Heron Reef also shown in **Figure 5B**. In contrast, the θ_v profiles for the 22 February indicate a statically neutral lower atmosphere in which the influence of Heron Reef is masked by the arrival of a monsoon airmass and associated increase in wind speed (**Figure 6C**). On the 23 February, the tethersonde profiles (**Figure 6D**) show the lower atmosphere became increasingly stable with cooling at the surface corresponding to increased cloud cover, reduced solar heating of the reef and down mixing of cooler air associated with convective showers. Satellite imagery from the 22 and 23 February 2009 show extensive high-level cirrus and cirrostratus cloud over the southern GBR with lower-level cumulus.

Desert Bordering Coral Reefs – Case Study Gulf of Eilat

EC measurements over the fringing coral reefs in the northwest GoE were made by instrumentation located on the shore as shown in **Figure 1C**. The EC system consisted of a RM Young 81000 3D sonic anemometer, Li-Cor 7500 open path gas analyser, Kipp and Zonen CNR1 radiometer, and ancillary sensors installed at the shoreline 2.5 m above mean sea level on the pier of Eilat's Coral World Underwater Observatory (29° 30'15.43" N, 34°55'6.68" E). Sensors were controlled by Campbell Scientific CR1000X dataloggers and regularly serviced with the Li-Cor 7500 open path gas analysers washed to ensure the optical sensors were free of salt and dust. The measurement footprint of the EC extended over corals in water depths from 0 m to 40 m. Simple linear interpolation was used to fill gaps where 1 data point was missing or where a data spike or unrealistic change in sign of energy flux had occurred. Longer gaps in data were filled using EC data from a nearby site (Abir et al., 2022) when that EC measurement footprint also extended over the fringing coral reef. A 3-point simple moving average was then applied to the EC data.

Air – Sea Exchanges During Hot and Dry Conditions

The 6 - 10 September 2020 was characterised by a broad area of lower atmospheric pressure and a weak synoptic pressure gradient over the Gulf of Eilat associated with the Persian Trough, while a ridge of high pressure was located over the western Mediterranean. This resulted in clear skies and northerly winds over the field site which peaked daily around 0900 IST (Israel Standard Time - UTC + 2 hrs) at 7 to 8 ms^{-1}.

The surface energy balance for this period shows Q* peaking daily under cloudless skies at around 800 W m^{-2} (**Figure 7A**). Latent heat flux peaked on the 6 and 7 September at ~500 W m^{-2} and then gradually trended lower toward the 10 September. Sensible heat flux was mostly negative associated with heat transfer from the air to the

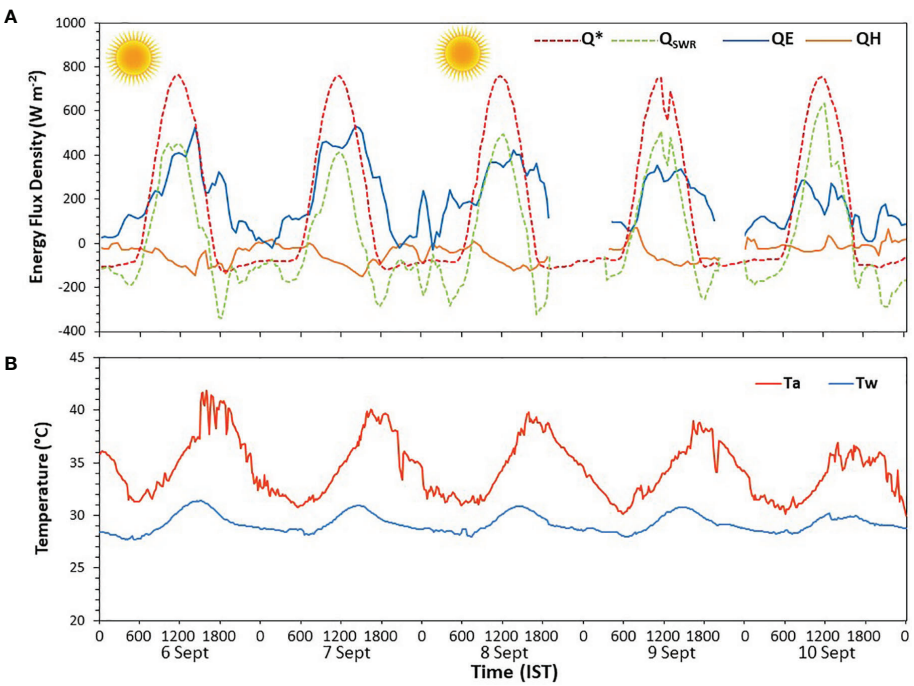

FIGURE 7 | Eddy covariance energy flux measurements (6 - 10 September 2020) made over the desert fringing coral reef at Eilat (**Figures 1A-C**) **(A)**; and corresponding water and air temperatures **(B)**.

water, while Q_{swr} peaked around midday, becoming more significant over the 5-day period (**Figure 7A**).

Throughout the 5-day period the temperature of the water overlying the fringing coral reef displayed a diurnal cycle ranging from a minimum of 27.8°C to a maximum of 31.2°C with no discernible warming/cooling trend (**Figure 7B**). Daily maximum Ta ranged from ~36°C to ~41°C with minimums of ~31°C (**Figure 7B**). These conditions resulted in a strong surface-based temperature inversion overlying the coral reef, while aerological profiles created using reanalysis data (NCEP operational Global Forecast System analysis data) displayed a stable layer over the GoE extending up to at least 800 m asl. As a result, the high positive daytime Qe flux transfers (evaporation) from the water to the air did not result in the formation of cloud, indicated in the Q* record (**Figure 7A**) as convection was supressed.

DISCUSSION

Coral reefs present distinct and typically abrupt changes in the thermal and dynamic properties of tropical and subtropical oceans. Direct measurements of air-sea exchanges of energy over coral reefs are essential to develop understanding of the influence coral reefs have on meteorology through exchanges of heat, moisture, and momentum with the atmosphere. Exchanges of Qe and Qh for example, influence thermodynamic processes in the atmospheric boundary-layer which may include winds, convection, cloud, and precipitation. The warmth of shallow waters overlying coral reefs and the formation of unstable CRLs may act to enhance vertical motion and dispersion of biogenic aerosols including the aerosol precursor gas DMS, salt, and moisture. However, direct measurements of air-sea energy exchanges over coral reefs and the local meteorology are rare, while the aerological profiles made at Heron Reef are unique (MacKellar et al., 2012b). Here we have presented selected new examples of summertime measurements of air-sea energy exchanges and profiles of the thermodynamic structure of the lower atmosphere over Heron Reef, GBR and, initial energy balance measurements from the desert fringing coral reefs in the GoE.

Humid Tropical/Subtropical Coral Reefs

EC measurements made during summer fair weather and monsoon conditions at Heron Reef showed the majority of available net radiant energy is partitioned into Q_{swr}. This raised the temperature of water overlying the reef resulting in the formation of a warm, humid, and unstable CRLs ~60 to ~100 m asl. (**Figures 3**–**6**) embedded within the MBL, which in case study 2 (20 - 23 February 2009) was ~600 to ~900 m in depth. The boundary at the top of the MBL, i.e., the entrainment zone, was clearly identified in ceilometer backscatter data indicating a sharp change in humidity (Flamant et al., 1997). As a result, under humid summer conditions coral reefs can modify the lower atmosphere resulting in the formation of an unstable CRL. This we believe contributed to formation of cumulus clouds following heating of the reef throughout late morning and early afternoon resulting in precipitation on the 4 February 2008. That is, the daily peak in radiative warming of reef SST and air–sea fluxes (early afternoon) invigorate convection leading to daily maximum cumulus in the late afternoon (Ruppert and Johnson, 2016).

While cloud height was only measured during 20 - 23 February 2009 and found to occur near the top of the MBL (and above), it's likely that the warmth of the reef and release of Qe associated with convective cloud formation may have contributed to onset of cumulus indicating more unstable conditions (**Figures 2B, C**). Cloud above the MBL as shown in **Figure 2B** and observed in case study 2 by ceilometer (**Figures 5B–D**) was likely caused by broader scale synoptic conditions. During case study 2, the MBL became more humid as seen in **Figure 5** indicated by the pronounced increase in reflectivity in **Figure 5D** (Dupont et al., 1994; Flamant et al., 1997). This increase in reflectivity may have also been in-part a result of increased biogenic aerosol concentrations (Schlosser et al., 2020) but without direct *in-situ* sampling this cannot be confirmed. Precipitation was identified by the ceilometer falling from cloud near the top of the MBL and from heights of 3000 to 4000 m asl (**Figure 5D**). Vertical profiles of $\theta_v$during case study 2 show on the 20 -21 February 2009 the CRL became more unstable through the morning and afternoon before onset of cooling in the late afternoon (**Figures 6A–C**). On the 23 Feb 2009 the $\theta_v$profiles show the lower atmosphere becoming stable with the lowest ~300 m cooling (**Figure 6D**) in response to likely down mixing of cooler air from aloft toward the surface with precipitation (**Figure 5D**). This sequence is like that reported by Ruppert and Johnson (2015) for days leading up to the onset of convection over warm SSTs in the Indian Ocean associated with the Madden Julian Oscillation. Namely, the diurnally forced convection that occurs in response to daytime peaks in SST and air–sea fluxes (Qe) over warm seas, initially under clear skies, increases humidity in the lower atmosphere and invigorates moist convection by reducing convective inhibition (Ruppert and Johnson, 2015). By the 23 Feb 2009 at Heron Reef such a sequence of events over the reef and adjacent sea led to periods of heavy convective rainfall (**Figure 6D**).

MacKellar et al. (2012b; 2013) presented results from the only other study that has made direct measurements of both air-sea energy exchanges over a coral reef (Heron Reef) and the CRL. They identified the CRL using vertical profiles of virtual potential temperature (θ_v) and mixing ratio (q) obtained from kite tethersonde soundings. Ceilometer data were used also to identify the mixed layer height with the addition of radiosonde soundings. The CRL was observed to reach a maximum height of approximately 135 m above sea level (asl.) in mid-afternoon (summer) with background mixed layer depths ranging from around 450 m to 2500 m depending on prevailing synoptic conditions. These observations are like those presented here for the summer case studies although MBL depths on occasions were greater. This likely reflects MacKellar's use of radiosondes providing direct measurements of temperature, and different prevailing synoptic meteorology. MacKellar et al. (2013)

highlighted similarities of the CRL observed at Heron Reef with CIBLs found downwind over the warm side of ocean fronts such as the Gulf Stream and Kuroshio extension, east of Japan. At such locations warmer SSTs initiate CIBL development within the mixed layer and cloud formation which on occasions may cause precipitation (Small et al., 2008). Over coral reefs such as Heron Reef, the CRL plume is likely to extend downwind similar to the CIBLs observed downwind of warm ocean currents (Hsu, 1984; Small et al., 2008).

Subtropical Desert Coral Reefs

In contrast to the warm humid setting of Heron Reef on the GBR, the EC measurements from over the desert fringing coral reefs in the GoE highlight the significant Qe fluxes associated with evaporation during the day and night. Q_{swr} is still very substantial in this arid location displaying a generally similar diurnal signal to Heron Reef. Accordingly, evaporation from water overlying the coral reefs at the GoE is the primary process by which energy is lost from the reef to the air (Abir et al., 2022). As a result, there was no net increase in water temperature from the 6 – 10 September 2020, although the diurnal range decreased slightly over the 5 days (**Figure 7A**). Notably, air temperature remained much higher than the water temperature, thereby causing a very stable layer of air over the coral reef. Stable internal boundary layers have been observed in other locations where warm air blows offshore over cool/cold sea surface as reported by Garratt and Ryan (1989) over the coast of southern Australia; Mahrt et al. (2016) Atlantic Ocean, Massachusetts and Grachev et al. (2018) on the North Carolina coast. Stable stratification generated in the GoE by warm-air advection and evaporation over coral reefs inhibit vertical motion at the surface. This stable layer was part of a deeper temperature inversion associated with the regional meteorology that was around 800 m deep.

Temperature inversions as observed in the GoE impede vertical motion in the atmosphere and cloud did not form. While no direct measurements of vertical profiles of temperature and humidity were made in the GoE we believe that in such a setting where water temperature remains well below air temperature, vertical dispersion of aerosols, moisture and DMS are unlikely. Instead, they will be advected downwind where they disperse in the dry atmosphere.

Coupling to the Atmospheric Boundary Layer

The case studies presented here show that coral reefs in humid climates may effectively couple to the overlying atmosphere influencing its thermodynamic properties impacting cloud and possibly precipitation. The coupling was observed to occur *via* convective exchange leading to formation of a CRL within the MBL. Leahy et al. (2013) using *in-situ* sea surface temperature measurements and satellite cloud field observations from the central GBR found cloud cover explaining up to 32.1% of variation in SST with the greatest effect during summer. Accordingly, our observations from Heron Reef begin to shed light on the possible role of coral reefs in this cloud formation over the GBR i.e., as coral reefs warm, they initiate convection triggering cloud formation under favourable synoptic conditions such as occur during the summer monsoon. In contrast, under settled summer El Niño conditions when the atmosphere is more stable over the GBR, cloud development may be suppressed resulting in extreme heating of water overlying coral reefs causing bleaching (McGowan and Theobald, 2017; Zhao et al., 2021).

In contrast, the case study from the GoE suggests that coral reefs in hot arid environments may remain decoupled from the overlying atmosphere as a result of strong surface-based temperature inversions. Such inversions inhibit vertical exchange of heat, moisture and aerosols and would contribute to inhibiting cloud development that would otherwise lower receipt of solar radiation over the reef. In these environments, observations from the fringing coral reefs in the GoE highlight the importance of Qe in protecting coral from heatwaves and associated coral bleaching (Abir et al., 2022).

CONCLUSION

Understanding exchanges of energy, moisture, momentum, and gases across the air-sea interfacial boundary on coral reefs and the influence on the atmosphere is critical to inform debate on future impacts of climate change on coral reefs. It is not scientific to assume that correlations are evidence enough of causality or to simplify complex cause – effect relationships because they align with socially and/or politically attractive narratives on the relationships between coral reefs – meteorology and climate. Direct measurements of the meteorology of coral reefs including energy exchanges across the air-sea interface and associated coupling to the lower atmosphere are therefore essential to inform such debate from which evidence-based policy to mitigate risks to coral reefs including from global warming can be developed.

Here we have presented through case study direct measurements of air-sea energy exchanges over coral reefs in two profoundly different climatic zones. These measurements show that under summertime conditions coral reefs in humid tropical/subtropical environments may couple to the lower atmosphere through exchange of heat, moisture, and momentum. This leads to the formation of CRLs within the lower levels of the MBL providing a mechanism for coral reefs to influence cloud, and possibly precipitation through convective exchange with the lower atmosphere. In contrast, our case study from the northern GoE in the Red Sea shows that where air overlying coral reefs is much warmer than the water temperature, stable stratification of the lower atmosphere will inhibit vertical motion and therefore, convective cloud development. In such different climatic regions, convection over coral reefs such as those in the GBR would be a possible mechanism by which aerosols and pre-curser aerosol gases such as DMS could be carried into the atmosphere, while in hot arid desert environments, a stable layer over corals reefs impedes such transport.

The research presented and cited in this article provides initial insights to coral reef meteorology and begins to shed

light on the interactions between coral reefs and broader scale meteorology. However, substantial knowledge gaps remain around seasonal variability in coral reef – atmosphere coupling and potential feedback mechanisms. While the works of Fiddes et al., 2022 question the role of coral reef bioclimatic links through coral reef emitted DMS in cloud microphysics, coral-reef forced convection may provide a possible mechanism for a DMS signal in cloud fields over reefs. Accordingly, future research is strongly recommended that combines direct measurement of the surface energy exchanges over coral reefs and atmospheric thermodynamics with aerosol profile sampling including within clouds. This should be combined with numerical modelling to provide data sets to nudge and validate model runs and to inform future direct measurement field research.

DATA AVAILABILITY STATEMENT

The raw data supporting the conclusions of this article will be made available by the authors, without undue reservation.

AUTHOR CONTRIBUTIONS

HM and MS conceived and conducted research at Heron Island. HM, NL, and SA conceived and conducted research at Eilat. All authors were involved with data analysis. HM wrote the manuscript with contributions from NL and SA. All authors contributed to the article and approved the submitted version.

ACKNOWLEDGMENTS

The authors acknowledge the support of their host institutions: The University of Queensland, Geological Survey of Israel, Hebrew University of Jerusalem, and The Inter-University Institute for Marine Sciences. We thank the Dead Sea Observatory team members Uri Malik, Guy Tau and Ziv Mor for their assist in the field, Adrien Guyot for processing the LiDAR data from Heron Island, and Yoni Shaked for assistance and discussions. The research was supported by funding from the Australia-Israel Cooperation in Science - Zelman Cowen Academic Initiatives (ZCAI), PIs – HM and NGL, and by the Israel Science Foundation (grant # ISF-2018/1471), PI – NGL.

REFERENCES

Abir, S., McGowan, H. A., Shaked, Y., and Lensky, N. G. (2022). Identifying an Evaporative Thermal Refugium for the Preservation of Coral Reefs in a Warming World - The Gulf of Eilat (Aqaba). *J. Geophys. Res. Atmos.*

Alpert, P., Abramsky, R., and Neeman, B. (1990). The Prevailing Summer Synoptic System in Israel–Subtropical High, Not Persian Trough. *Israel J. Earth Sci.* 39 (2), 93–102.

Bitan, A., and Sa'Aroni, H. (1992). The Horizontal and Vertical Extension of the Persian Gulf Pressure Trough. *Int. J. Climatol.* 12 (7), 733–747. doi: 10.1002/joc.3370120706

Broadbent, A., and Jones, G. (2006). Seasonal and Diurnal Cycles of Dimethylsulfide, Dimethylsulfoniopropionate and Dimethylsulfoxide at One Tree Reef Lagoon. *Environ. Chem.* 3, 260–267. doi: 10.1071/EN06011

Carlson, D. F., Fredj, E., Gildor, H., Biton, E., Steinbuck, J. V., Monismith, S. G., et al. (2012). Observations of Tidal Currents in the Northern Gulf of Eilat/Aqaba (Red Sea). *J. Marine Syst.* 102–104, 14–28. doi: 10.1016/j.jmarsys.2012.04.008

Charlson, R. J., Lovelock, J. E., Andreae, M. O., and Warren, S. G. (1987). Oceanic Phytoplankton, Atmospheric Sulphur, Cloud Albedo and Climate. *Nature* 326, 655–661. doi: 10.1038/326655a0

Chen, D., and Krol, A. (1997). "Hydrogeology of Heron Island, Great Barrier Reef, Australia", in Geology and Hydrogeology of Carbonate Islands. Developments in Sedimentology. *Eds. H. L. Vacher and T. Quinn* (New York: Elsevier Science), 867—884.

Clayson, C. A., and Edson, J. B. (2019). Diurnal Surface Flux Variability Over Western Boundary Currents. *Geophys. Res. Lett.* 46, 9174–9182. doi: 10.1029/2019GL082826

Cropp, R., Gabric, A., van Tran, D., Jones, G., Swan, H., and Butler, H. (2018). Coral Reef Aerosol Emissions in Response to Irradiance Stress in the Great Barrier Reef, Australia. *Ambio* 47 (6), 671–681. doi: 10.1007/s13280-018-1018-y

Dupont, E., Pelon, J., and Flamant, C. (1994). Study of the Moist Convective Boundary Layer Structure by Backscatter Lidar. *Bound Lay. Meteorol.* 69, 1–25. doi: 10.1007/BF00713292

Fiddes, S. L., Woodhouse, M. T., Lane, T. P., and Schofield, R. (2021a). Coral-Reef-Derived Dimethyl Sulfide and the Climatic Impact of the Loss of Coral Reefs. *Atmos. Chem. Phys.* 21, 5883–5903. doi: 10.5194/acp-21-5883-2021

Fiddes, S., Woodhouse, M., Utembe, S., Schofield, R., Alroe, J., Chambers, S., et al. (2022). The Contribution of Coral Reef-Derived Dimethyl Sulfide to Aerosol Burden Over the Great Barrier Reef: A Modelling Study. *Atmos. Chem. Phys. Discuss.* 22, 2419–2445. doi: 10.5194/acp-22-2419-2022

Flamant, C., Pelon, J., Flamant, P. H., and Durand, P. (1997). Lidar Determination of the Entrainment Zone Thickness at the Top of the Unstable Marine Atmospheric Boundary Layer. *Bound Lay. Meteorol.* 83, 247–284. doi: 10.1023/A:1000258318944

Garratt, J. R. (1990). The Internal Boundary Layer — A Review. *Bound Lay. Meteorol.* 50, 171–203. doi: 10.1007/BF00120524

Garratt, J. R. (1994). Review: The Atmospheric Boundary Layer. *Earth Sci. Rev.* 37, 89–134. doi: 10.1016/0012-8252(94)90026-4

Garratt, J. R., and Ryan, B. F. (1989). The Structure of the Stably Stratified Internal Boundary-Layer in Offshore Flow Over the Sea. *Bound Lay. Meteorol.* 47 (1), 17–40. doi: 10.1007/BF00122320

Golbazi, M., and Archer, C. L. (2019). Methods to Estimate Surface Roughness Length for Offshore Wind Energy. *Adv. Meteorol.* 2019, 5695481. doi: 10.1155/2019/5695481

Gourlay, M. R. (1988). "Coral Cays' Products of Wave Action and Geological Processes in a Biogenic Environment," in *Proc. 6th Int. Coral Reef Symposium, Great Barrier Reef Committee, Townsville, Australia*. 491–496.

Grachev, A. A., Leo, L. S., Fernando, H. J. S., Fairall, C. W., Creegan, E., Blomquist, B. W., et al. (2018). Air–Sea/Land Interaction in the Coastal Zone. *Bound Lay. Meteorol.* 167, 181–210. doi: 10.1007/s10546-017-0326-2

He, Y., Fu, J., Chan, P. W., Li, Q., Shu, Z., and Zhou, K. (2021). Reduced Sea-Surface Roughness Length at a Coastal Site. *Atmosphere* 12, 991. doi: 10.3390/atmos12080991

Hsu, S. A. (1984). Effect of Cold-Air Advection on Internal Boundary-Layer Development Over Warm Ocean Currents. *Dyn. Atmos. Oceans* 8, 307–319. doi: 10.1016/0377-0265(84)90015-0

Kotthaus, S., O'Connor, E., Münkel, C., Charlton-Perez, C., Haeffelin, M., Gabey, A. M., et al. (2016). Recommendations for Processing Atmospheric Attenuated Backscatter Profiles From Vaisala CL31 Ceilometers. *Atmos. Meas. Tech.* 9, 3769–3791. doi: 10.5194/amt-9-3769-2016

Leahy, S. M., Kingsford, M. J., and Steinberg, C. R. (2013). Do Clouds Save the Great Barrier Reef? Satellite Imagery Elucidates the Cloud-SST Relationship at the Local Scale. *PloS One* 8 (7), e70400. doi: 10.1371/journal.pone.0070400

MacKellar, M. C., McGowan, H. A., and Phinn, S. R. (2012a). Spatial Heterogeneity of Air-Sea Energy Fluxes Over a Coral Reef, Heron Reef, Australia. *J. Appl. Meteorol. Clim.* 51, 1353–1370. doi: 10.1175/JAMC-D-11-0120.1

MacKellar, M. C., McGowan, H. A., and Phinn, S. R. (2013). An Observational Heat Budget Analysis of a Coral Reef, Heron Reef, Great Barrier Reef, Australia. *J. Geophys. Res. Atmos.* 118 (6), 2547–2559. doi: 10.1002/jgrd.50270

MacKellar, M. C., McGowan, H. A., Phinn, S. R., and Soderholm, J. S. (2012b). Observations of Surface Energy Fluxes and Boundary-Layer Structure Over Heron Reef, Great Barrier Reef, Australia. *Bound Lay. Meteorol.* 146 (2), 319–340. doi: 10.1007/s10546-012-9767-9

Mahrt, L. (2000). Surface Heterogeneity and Vertical Structure of the Boundary Layer. *Bound Lay. Meteorol.* 96, 33–62. doi: 10.1023/A:1002482332477

Mahrt, L., Andreas, E. L., Edson, J. B., Vickers, D., Sun, J., and Patton, E. G. (2016). Coastal Zone Surface Stress With Stable Stratification. *J. Phys. Oceanogr.* 46 (1), 95–105. doi: 10.1175/JPO-D-15-0116.1

McGowan, H. A., Sturman, A. P., Mackellar, M. C., Weibe, A. H., and Neil, D. T. (2010). Measurements of the Surface Energy Balance Over a Coral Reef Flat, Heron Island, Southern Great Barrier Reef, Australia. *J. Geophys. Res. Atmos.* 15 (D19), D19124-1-D19124-12. doi: 10.1029/2010JD014218

McGowan, H., Sturman, P., Saunders, M., Theobald, A., and Wiebe, A. (2019). Insights From a Decade of Research on Coral Reef – Atmosphere Energetics. *J. Geophys. Res. Atmos.* 124 (8), 4269—4282. doi: 10.1029/2018JD029830

McGowan, H., and Theobald, A. (2017). ENSO Weather and Coral Bleaching on the Great Barrier Reef, Australia. *Geophys. Res. Lett.* 44 (20), 10,601—10,607. doi: 10.1002/2017GL074877

Ruppert, J. H.Jr., and Johnson, R. H. (2015). Diurnally Modulated Cumulus Moistening in the Pre-Onset Stage of the Madden–Julian Oscillation During DYNAMO. *J. Atmos. Sci.* 72 (4), 1622–1647. doi: 10.1175/JAS-D-14-0218.1

Ruppert, J. H. Jr., and Johnson, R. H. (2016). On the Cumulus Diurnal Cycle Over the Tropical Warm Pool. *J. Adv. Model. Earth Syst.* 8, 669–690. doi: 10.1002/2015MS000610

Schlosser, J. S., Dadashazar, H., Edwards, E.-L., Hossein Mardi, A., Prabhakar, G., Stahl, C., et al. (2020). Relationships Between Supermicrometer Sea Salt Aerosol and Marine Boundary Layer Conditions: Insights From Repeated Identical Flight Patterns. *J. Geophys. Res. Atmos.* 125, e2019JD032346. doi: 10.1029/2019JD032346

Shaked, Y., and Genin, A. (2019). *Gulf of Eilat National Monitoring Report 2017* (Eilat, Israel: Israel Ministry of Environmental Protection), 209p.

Shaked, Y., and Genin, A. (2020). *Gulf of Eilat National Monitoring Report 2019* (Eilat, Israel: Israel Ministry of Environmental Protection), 187p.

Small, R. J., DeSzoeke, S. P., Xie, S. P., O'Neill, L., Seo, H., Song, Q., et al. (2008). Air-Sea Interaction Over Ocean Fronts and Eddies 2008. *Dyn. Atmos. Oceans* 45 (3–4), 274–319. doi: 10.1016/j.dynatmoce.2008.01.001

Swan, H. B., Crough, R. W., Vaattovaara, P., Jones, G. B., Deschaseaux, E. S. M., Eyre, B. D., et al. (2016). Dimethyl Sulfide and Other Biogenic Volatile Organic Compound Emissions From Branching Coral and Reef Seawater: Potential Sources of Secondary Aerosol Over the Great Barrier Reef. *J. Atmos. Chem.* 73, 303–328. doi: 10.1007/s10874-016-9327-7

Vickers, D., Mahrt, L., Sun, J., and Crawford, T. (2001). Structure of Offshore Flow. *Mon. Weather Rev.* 129 (5), 1251–1258. doi: 10.1175/1520-0493(2001)129<1251:SOOF>2.0.CO;2

Woodroffe, C. D. (2003). *Coasts: Form, Process and Evolution* (New York.: Cambridge Univ. Press), 623p.

Zhao, W., Huang, Y., Siems, S., and Manton, M. (2021). The Role of Clouds in Coral Bleaching Events Over the Great Barrier Reef. *Geophys. Res. Lett.* 48, e2021GL093936. doi: 10.1029/2021GL093936

Conflict of Interest: The authors declare that the research was conducted in the absence of any commercial or financial relationships that could be construed as a potential conflict of interest.